Kinetics and mechanism of oxidative cleavage of the metal–metal bond in $[M_2(CO)_{10}]^{2-}$, M = Cr, Mo and W

Julia R. Phillips and William C. Trogler*
Department of Chemistry, University of California, San Diego, La Jolla, CA 92093-0506 (USA)

Abstract

Electrochemically-induced metal–metal bond cleavage in $[M_2(CO)_{10}]^{2-}$ (M = Cr, Mo, W) has been studied using cyclic voltammetry, bulk electrolysis and double potential step chronocoulometry. Metal–metal bond homolysis, which occurs on oxidation in THF, can be modeled with an EC second-order disproportionation mechanism. The key step involves reaction of $2[M_2(CO)_{10}]^{\cdot-}$ to form $[M_2(CO)_{10}]^{2-}$ and $M(CO)_5(THF)$. Electron transfer rate constants for the homogeneous disproportionation step, k_d, were determined by double potential step chronocoulometry: $2.5 \pm 0.1 \times 10^3$ M^{-1} s^{-1} for $[W_2(CO)_{10}]^{\cdot-}$ and $5.9 \pm 0.3 \times 10^2$ M^{-1} s^{-1} for $[Mo_2(CO)_{10}]^{\cdot-}$ in THF at 20.0 °C. The $[Cr_2(CO)_{10}]^{\cdot-}$ radical underwent disproportionation too slowly to observe at room temperature, but a value of $k_d \leqslant 1.7 \times 10^2$ M^{-1} s^{-1} was estimated to be the upper limit of the rate constant at 35.0 °C. Activation parameters for k_d were determined. For $[Mo_2(CO)_{10}]^{\cdot-}$, $\Delta H^{\ddagger} = 6.9 \pm 0.5$ kcal mol^{-1} and $\Delta S^{\ddagger} = -22.4 \pm 1.9$ cal K^{-1} mol^{-1}. For $[W_2(CO)_{10}]^{\cdot-}$, $\Delta H^{\ddagger} = 3.3 \pm 0.5$ kcal mol^{-1} and $\Delta S^{\ddagger} = -31.7 \pm 0.5$ cal K^{-1} mol^{-1}. The relative reactivities of the radicals W > Mo ≫ Cr parallel the driving force for electron transfer, as measured by the potential difference for the oxidation of $[M_2(CO)_{10}]^{2-}$ and $[M_2(CO)_{10}]^{\cdot-}$. The k_d step is proposed to involve outer-sphere electron transfer.

Introduction

The reactivity of transition metal–carbonyl dimers centers around cleavage of the metal–metal bond. Homolytic metal–metal bond cleavage is well-known to result in the formation of highly reactive seventeen-electron organometallic radicals. Radicals are frequently generated from these systems by photochemical means [1–6], but some electrochemical studies of such dimers (and the corresponding monomers) have been reported [7–14]. Few electrochemical studies have investigated the kinetics of metal–metal bond cleavage that occurs as electrons are removed from or added to the metal-based d-orbitals [7, 8]. The successive removal of electrons to break a metal–metal single bond [15] might be one way to study this process; however, attempts to oxidize dinuclear metal carbonyls not constrained by bridging ligands generally leads to irreversible two-electron oxidation processes.

In previous studies of bridged dinuclear radicals, such as $Fe_2(CO)_7(\mu\text{-}PPh_2)$ [16], we found a high susceptibility of the complex to undergo nucleophilic attack. Therefore, the high instability of $[M_2(CO)_{10}]^{\cdot+}$ species for M = Mn or Re might arise because of high susceptibility to nucleophile-induced metal–metal bond cleavage for the cationic species. For these reasons isoelectronic anions were examined, which might give longer lived radicals. Herein, we report the oxidation of $[M_2(CO)_{10}]^{2-}$ (M = Cr, Mo, W) to produce singly oxidized binuclear radicals. By varying the time scale of measurement, irreversible two-electron oxidative cleavage of the metal–metal bond can be observed and shown to arise from a homogeneous disproportionation mechanism, which proceeds by outer-sphere electron transfer between two $[M_2(CO)_{10}]^{\cdot-}$ species.

Experimental

General

All manipulations were performed under a nitrogen atmosphere using standard Schlenk techniques or in a Vacuum Atmospheres glove box. Care was taken to exclude light from solutions of the dinuclear metal carbonyls. THF was dried over potassium and distilled just before use. Acetonitrile and dichloromethane were dried over CaH_2 and stored under nitrogen after distillation. Pyridine was dried over sodium, distilled, and stored under nitrogen. Tetrabutylammonium perchlorate (TBAP) was recrystallized from ethyl acetate/isooctane, dried *in vacuo*, and stored under nitrogen. $[PPN]_2[M_2(CO)_{10}]$ (M = Cr, Mo, W) were synthesized

*Author to whom correspondence should be addressed.

0020-1693/92/$5.00

using the method of Ruff and Schlientz [17]. $M(CO)_6$ and [PPN]Cl were obtained from commercial sources and used as received. Triphenylphosphine was used as received from commercial sources. Samples of $M(CO)_5Cl^-$ were generously provided by Mr Richard Heyn. FT-IR spectra were recorded on an IBM IR/32 spectrometer.

Electrochemical measurements

Electrochemical studies employed a BAS-100 electrochemical analyzer equipped with a Houston Instruments HMP-40 digital plotter. For cyclic voltammetry and double potential step chronocoulometry experiments, a locally-constructed Schlenk cell, equipped with a Pt disk working electrode (diameter ~0.5 mm), a Pt wire auxiliary electrode, and either an $Ag/AgNO_3$ reference or an Ag wire pseudo-reference electrode, was used. The cell was placed in a Brinkman-Lauda RMS constant temperature circulating bath for the variable temperature studies. Bulk electrolysis was conducted in a three-compartment Schlenk cell that had medium fritted glass disks separating the compartments. The cell was fitted with a Pt gauze working electrode, a Pt wire auxiliary electrode, and an $Ag/AgNO_3$ reference or an Ag wire pseudo-reference electrode.

Typical procedures

For all experiments, a background cyclic voltammogram was recorded of the solvent containing TBAP only (0.1 M unless otherwise noted). For cyclic voltammetry and double potential step chronocoulometry measurements, 10 ml of the TBAP solution containing the dimer (0.001 M unless otherwise noted) was used in the cell. For bulk electrolysis, 10 ml of a similar solution was used in the center (working) cell compartment, with TBAP electrolyte only in the solutions for the other two compartments. Before double potential step measurements with the Ag wire reference it was necessary to cycle about the $[M_2(CO)_{10}]^{2-}$ oxidation wave several times until the potential drift stopped. For each chronocoulometric measurement the Q versus $t^{1/2}$ plots were examined to ensure that the data were not distorted by capacitive charging-solution resistance (and adsorption) problems. This limited data acquisition to pulse times longer than 30–50 ms.

Results and discussion

Cyclic voltammograms were recorded for the first and second oxidation waves of $[PPN]_2[M_2(CO)_{10}]$ (M = Cr (**1**), Mo (**2**), W (**3**)) in THF versus the $Ag/AgNO_3$ reference electrode; see Table 1 for the $E^{1/2}$ values. For **1**, the first oxidation was reversible at all scan rates between 50 and 2000 mV/s, while the corresponding oxidations for **2** and **3** were not reversible at scan rates below 500 and 1000 mV/s, respectively (see Fig. 1). The peak separation for the anodic and cathodic waves for the first oxidation process were very similar to ferrocene under the same conditions (Table

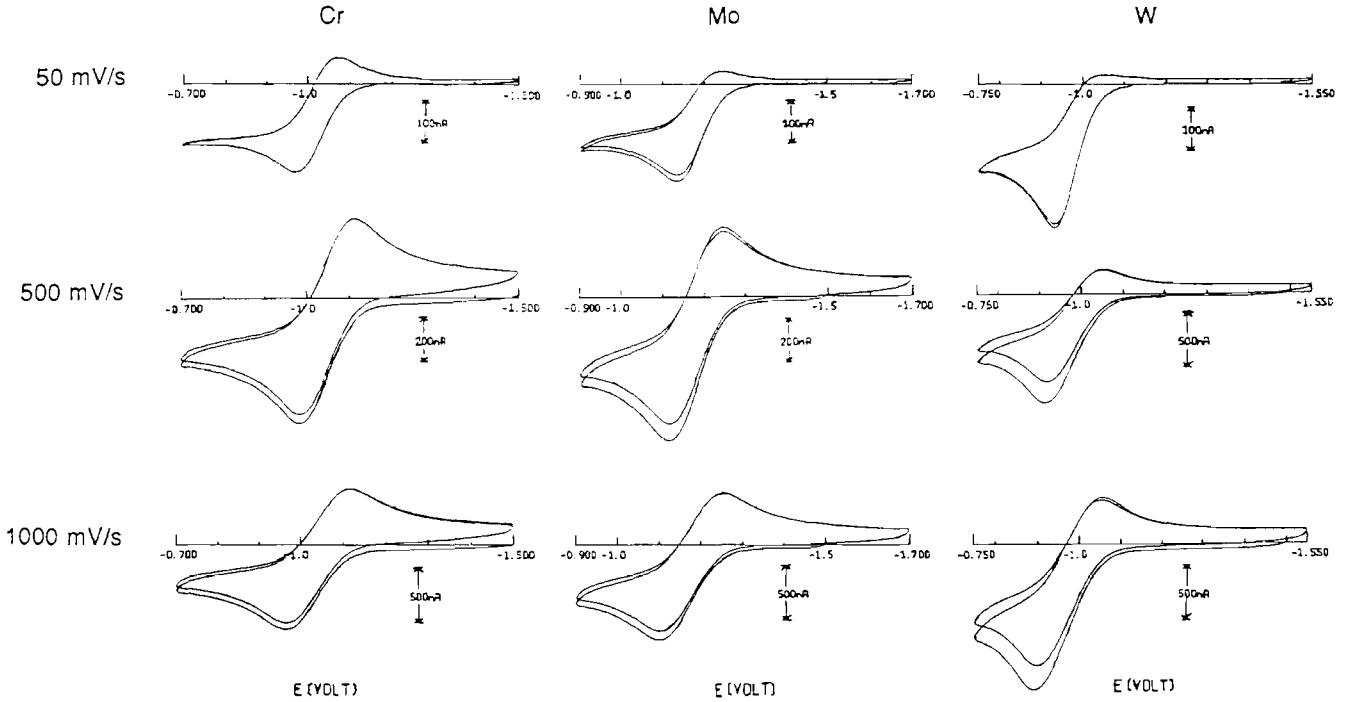

Fig. 1. Cyclic voltammograms of $[M_2(CO)_{10}]^{2-}$ in THF at various sweep rates.

TABLE 1. Potentials for the oxidation of $[M_2(CO)_{10}]^{2-}$ from cyclic voltammetry measurements at 100 mV/s[b]

Compound	E_{p1}^a (V)	E_{p1}^c (V)	$E^{1/2}$ (V)	E_{p2}^a (V)	$E_{p2}^a - E_{p1}^a$ (V)
$[Cr_2(CO)_{10}]^{2-}$ (1)	−0.975	−1.070	−1.025	−0.350	0.625
$[Mo_2(CO)_{10}]^{2-}$ (2)	−1.110	−1.210	−1.160	−0.625	0.485
$[W_2(CO)_{10}]^{2-}$ (3)	−0.900	−1.015	−0.960	−0.420	0.480
Cp_2Fe	+0.260	+0.020	+0.140		

[b]0.001 M solution of metal complex in THF; 0.1 M TBAP supporting electrolyte; $Ag/AgNO_3$ reference electrode.

1). Bulk electrolysis of **1**, **2** and **3** at −700, −900 and −750 mV, respectively (versus an $Ag/AgNO_3$ electrode), showed the oxidations to be net two-electron transfers in all cases. The products of bulk electrolysis were identified as $M(CO)_5(THF)$, by comparison of the FT-IR spectra of the bulk electrolysis solutions to the spectra of authentic samples of $M(CO)_5(THF)$ generated [18] by photolysis of $M(CO)_6$ in THF. Thus, the first oxidation wave of the $[M_2(CO)_{10}]^{2-}$ can either be a reversible one-electron process or an irreversible two-electron process, depending on the time scale of the experiment.

When excess (10 equiv.) of PPh_3 was added to the solutions just before bulk electrolysis, the result was again a net two-electron transfer in all cases. The IR spectra of the resulting solutions identified the products as being mostly $M(CO)_5(PPh_3)$ and some $M(CO)_4(PPh_3)_2$ (bulk electrolysis of **3**, Table 2, produced only the first product). The small amount of $M(CO)_4(PPh_3)_2$, detected in the IR spectrum, could arise if a $M(CO)_5^{\bullet -}$ or $M_2(CO)_{10}^{\bullet -}$ radical intermediate were labile toward CO substitution. Enhanced substitution in mono and dinuclear carbonyl radicals is known [19]. These results were consistent with the initial hypothesis, that electrochemically induced metal–metal bond cleavage proceeds by a simple ECE mechanism (shown in Scheme 1) in a fashion analogous to that proposed for $Mn_2(CO)_{10}$ [7].

ECE

$$[M_2(CO)_{10}]^{2-} \xrightarrow{-1e^-} [M_2(CO)_{10}]^{\bullet -}$$

$$[M_2(CO)_{10}]^{\bullet -} \xrightarrow{k} M(CO)_5^{\bullet -} + M(CO)_5$$

$$M(CO)_5^{\bullet -} \xrightarrow{-1e^-} M(CO)_5$$

$$M(CO)_5 \xrightarrow[THF]{fast} M(CO)_5THF \left(\xrightarrow[PPh_3]{fast} M(CO)_5(PPh_3) \right)$$

Scheme 1.

Double potential step chronocoulometry experiments were conducted with 10 equiv. of triphenylphosphine added. Since the study of a given solution may take several hours as pulse widths are varied, it seemed to help if any reactive $M(CO)_5(THF)$ was converted to stable $M(CO)_5(PPh_3)$. With added PPh_3, better reproducibility (±10%) in measured rates was obtained than when only THF was used. However, several experiments without added PPh_3 gave rates within 20% of those determined with added PPh_3. At room temperature, **2** and **3** reacted at a measurable rate, as evidenced by a drop in the charge ratios of between 0.2 and 0.35 as τ changed between 50 and 1000 ms (e.g. Fig. 2).

Several mechanisms in addition to the ECE process of Scheme 1 were considered as possible reaction pathways for oxidative cleavage of the metal–metal bond, and are shown in Scheme 2. These include ECEC,

TABLE 2. Bulk electrolysis data for $[M_2(CO)_{10}]^{2-}$ in THF[a]

Compound	Added reactant	n	Products
$[Cr_2(CO)_{10}]^{2-}$ (1)	THF only	1.7	$Cr(CO)_5(THF)$
	PPh_3	1.8	$Cr(CO)_5(PPh_3)$, $Cr(CO)_4(PPh_3)_2$
	CH_2Cl_2	1.3	$Cr(CO)_5(THF)$
$[Mo_2(CO)_{10}]^{2-}$ (2)	THF only	1.8	$Mo(CO)_5(THF)$
	PPh_3	1.7	$Mo(CO)_5(PPh_3)$, $Mo(CO)_4(PPh_3)_2$
	CH_2Cl_2	0.5	$Mo(CO)_5(THF)$, $Mo(CO)_5Cl^-$
$[W_2(CO)_{10}]^{2-}$ (3)	THF only	1.9	$W(CO)_5(THF)$
	PPh_3	1.8	$W(CO)_5(PPh_3)$
	CH_2Cl_2	1.2	$W(CO)_5(THF)$, $W(CO)_5Cl^-$

[a]0.001 M solution of metal complex; 0.05 M TBAP supporting electrolyte; 0.01 M triphenylphosphine; 0.15 M dichloromethane; $Ag/AgNO_3$ reference electrode.

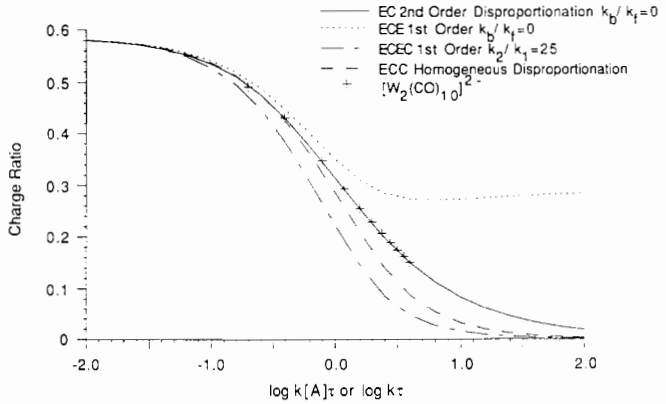

Fig. 2. Working curves and room temperature data for **3** in THF.

when k_2/k_1 is large; ECC homogeneous disproportionation, when k_2/k_1 is large; and EC second-order disproportionation, when k_b/k_f is 0. Since k_2 for the first two mechanisms is expected to be rapid and k_f is irreversible after $M(CO)_5$ is trapped by ligand, the limiting cases assumed are reasonable. The data were fit to the working curves that had been calculated for these mechanisms by Hanafey *et al.* [20]. The best fit with the smallest percentage error in the rate constant was clearly the EC second-order disproportionation mechanism. The working curves for the possible mechanisms and the fit of the room temperature data for **3** are shown in Fig. 2. Note that in the EC second-order disproportionation mechanism, the rate-determining step is not metal–metal bond cleavage, but electron transfer. The plausibility of this mechanism is further supported by the observation that the charge ratio data follows the EC second-order disproportionation working curve when the concentration of the dimer is varied. This mechanism requires that the rate of reaction be second order in the metal complex; a metal dimer concentration dependence quite different from the other possible mechanisms. Double potential step chronocoulometry data were collected for **2** and **3** at a series of temperatures with the cell immersed in a constant temperature bath. The rates calculated for the EC second-order disproportionation were used in Eyring plots to determine the activation parameters. The quantities are given in Tables 3 and 4. The rates, on the order of 1×10^3 M^{-1} s^{-1}, the low $\Delta H^{\ddagger}$ and the large negative $\Delta S^{\ddagger}$ are consistent with outer-sphere electron transfer being the rate-determining step [21].

The rate constants showed no appreciable change with a change in supporting electrolyte concentration, as shown for **3** in Table 5. This is expected in THF, since ion pairing should be nearly complete in a solvent with a low dielectric constant and no ionic strength dependence would be expected. For example, outer-sphere electron transfer between charged metallocenes in THF shows a similar lack of ionic strength effects [21]. The absence of any concentration dependence in the electrolyte, and the ideal behavior of the Q versus $t^{1/2}$ plots, also show that the data does not suffer from capacitive charging or solution resistance problems.

ECEC

$$[M_2(CO)_{10}]^{2-} \xrightarrow{-1e^-} [M_2(CO)_{10}]^{\cdot-}$$
$$[M_2(CO)_{10}]^{\cdot-} \xrightarrow{k_1} M(CO)_5 + M(CO)_5^{\cdot-}$$
$$M(CO)_5^{\cdot-} \xrightarrow{-1e^-} M(CO)_5$$
$$M(CO)_5 \xrightarrow[L]{k_2} M(CO)_5L$$

ECC homogeneous disproportionation

$$[M_2(CO)_{10}]^{2-} \xrightarrow{-1e^-} [M_2(CO)_{10}]^{\cdot-}$$
$$[M_2(CO)_{10}]^{\cdot-} \xrightarrow{k_1} M(CO)_5^{\cdot-} + M(CO)_5$$
$$2M(CO)_5^{\cdot-} \xrightarrow{k_2} [M_2(CO)_{10}]^{2-}$$

EC second-order disproportionation

$$[M_2(CO)_{10}]^{2-} \xrightarrow{-1e^-} [M_2(CO)_{10}]^{\cdot-}$$
$$2[M_2(CO)_{10}]^{\cdot-} \underset{k_b}{\overset{k_f}{\rightleftharpoons}} [M_2(CO)_{10}]^{2-} + 2M(CO)_5$$

Scheme 2.

TABLE 3. Rate constants for EC second-order disproportionation of $[Mo_2(CO)_{10}]^{\cdot-}$ and $[W_2(CO)_{10}]^{\cdot-}$ in THF

T (°C)	k_d (M^{-1} s^{-1})	
	$[Mo_2(CO)_{10}]^{\cdot-}$	$[W_2(CO)_{10}]^{\cdot-}$
1.0	$2.1\pm0.1\times10^2$	$1.6\pm0.1\times10^3$
10.5	$3.3\pm0.1\times10^2$	$2.0\pm0.1\times10^3$
20.0	$5.9\pm0.3\times10^2$	$2.5\pm0.1\times10^3$
30.0	$8.2\pm0.4\times10^2$	$3.2\pm0.1\times10^3$

TABLE 4. Activation parameters for $[Mo_2(CO)_{10}]^{\cdot-}$ and $[W_2(CO)_{10}]^{\cdot-}$ in THF

Compound	$\Delta H^{\ddagger}$ (kcal mol^{-1})	$\Delta S^{\ddagger}$ (cal K^{-1} mol^{-1})
$[Mo_2(CO)_{10}]^{\cdot-}$ (**2**)	6.9 ± 0.5	-22.4 ± 1.9
$[W_2(CO)_{10}]^{\cdot-}$ (**3**)	3.3 ± 0.15	-31.7 ± 0.5

TABLE 5. Rate constants for EC second-order disproportionation of $[W_2(CO)_{10}]^{\cdot-}$ at various supporting electrolyte concentrations[a]

[TBAP] (M)	k_d (M^{-1} s^{-1})
0.1	$3.4\pm0.2\times10^3$
0.2	$3.2\pm0.2\times10^3$
0.4	$3.5\pm0.4\times10^3$

[a]0.001 M solution of $[W_2(CO)_{10}]^{2-}$ in THF; 10 equiv. triphenylphosphine added; room temperature.

Double potential step chronocoulometry experiments were performed on **1**; however, the reaction proceeded much more slowly at room temperature than for **2** or **3**. In fact, the charge ratios showed essentially no change with a change in τ. A rate constant was measured by double potential step chronocoulometry at 35.0 °C in THF with a solution that was 0.002 M in **1**. The error in fitting these data was large (18%), but it does enable us to estimate the rate constant for disproportionation of $[Cr_2(CO)_{10}]^{\cdot -}$ as 1.7×10^2 M^{-1} s^{-1}. Because other kinetic processes may contribute at this elevated temperature, we conservatively regard this as an upper limit for the reactivity of $[Cr_2(CO)_{10}]^{\cdot -}$.

The fact that the reaction is much slower when the metal is Cr further supports the EC second-order disproportionation mechanism. Since the metal–metal bond in **1** is longer and weaker than those in **2** or **3** [22], then $[Cr_2(CO)_{10}]^{\cdot -}$ would be expected to react fastest if metal–metal bond cleavage was rate determining, and an ECE mechanism was operative. Thus, we have to look elsewhere to explain the reactivity ordering. The differences of potential between the first and second oxidations of **1**, **2** and **3** (see Table 1) indicate that electron transfer is thermodynamically uphill for the putative disproportionation step. This comparison must use the peak potential for the second irreversible oxidation; however, in the isostructural series the shift in this wave from its thermodynamic potential should be similar in all three compounds. Thus, the comparison of relative differences within the series should be valid. Also, note that the difference in the potentials is much larger for **1** than for **2** or **3**, and that the difference for **2** is only slightly larger than for **3**. These potential differences parallel the reactivity order for k_d $3>2\gg1$ in an inverse order. For outer-sphere electron transfer, Marcus theory predicts [23] that an increased potential barrier should decrease the reaction rate. Thus, the anomalous reactivity order we observe, where the third row metal reacts much more rapidly than the first row metal, makes sense in the context of the proposed mechanism and the observed redox potentials.

The possibility of a competing nucleophilic pathway for the radical intermediates was raised by the lack of reversibility in the cyclic voltammograms for **1**, **2** and **3** in acetonitrile. The first oxidation waves of **2** and **3** were completely irreversible at scan rates up to 5000 mV/s in acetonitrile, while the scan rate had to be at least 500 mV/s to see any reversibility for **1**. To investigate this further, cyclic voltammograms were recorded for THF solutions of **1** and **2** to which increasing amounts of pyridine or acetonitrile nucleophile had been added. Pyridine was added to the solutions until it equaled 10% of the total volume. No change in the reversibility of the oxidation of **1** or **2** was observed. When acetonitrile was added instead, the cyclic voltammograms of **1** and **2** were not changed appreciably until the acetonitrile volume totaled one-third that of the entire solution volume. Furthermore, double potential step chronocoulometry experiments performed on solutions of **1** in 100% acetonitrile and in 25/75 and 50/50 vol./vol. mixtures of THF/acetonitrile indicated that the same mechanism was operating (EC second-order disproportionation, see Fig. 3). The rate constant for **1** in acetonitrile alone is larger than that in 25/75 THF/acetonitrile or in 50/50 THF/acetonitrile, which is much larger than the (unmeasurable) rate constant for **1** in THF alone (see Table 6). These results suggest that a change in solvent polarity changes the electron-transfer rate, k_d, rather than changes the mechanism to nucleophilic attack at the radical dimer. In contrast to $Fe_2(CO)_7(\mu\text{-}PPh_2)$[16], and to mononuclear seventeen-electron radicals [24], the $[M_2(CO)_{10}]^{\cdot -}$ species are not especially susceptible to nucleophilic attack.

It is interesting to compare the electrochemical behavior of these Group 6 dimers to that of Group 5 analogues. The first oxidation wave of $Re_2(CO)_{10}$ occurs at +0.150 V, about 1 V more positive than the first oxidations for **1**, **2** or **3**. It is a completely irreversible process in both THF and acetonitrile at scan rates up to 1000 mV/s. The difference in oxidation potential is not surprising, since it should be more difficult to remove an electron from a neutral compound than from an

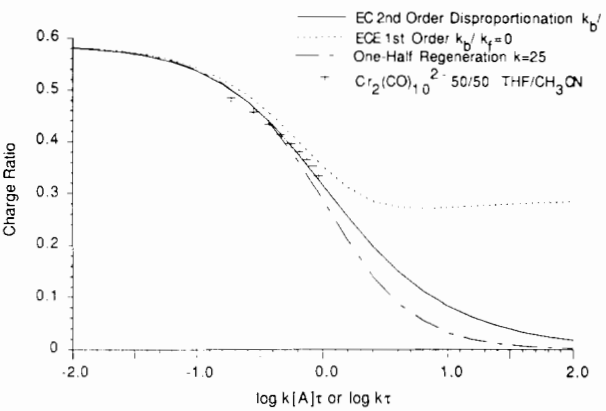

Fig. 3. Working curves and room temperature data for **1** in 50/50 THF/acetonitrile.

TABLE 6. Rate constants for EC second-order disproportionation of $[Cr_2(CO)_{10}]^{\cdot -}$ in various mixtures of THF and acetonitrile

CH_3CN[a] (%)	k_d (M^{-1} s^{-1})
100	$3.5\pm0.5\times10^3$
75	$2.2\pm0.3\times10^3$
50	$9.3\pm1\times10^2$
25	[b]

[a]Balance of solvent, THF; 0.1 M TBAP supporting electrolyte. [b]Too slow to measure.

anionic one. The irreversibility, when compared to **1**, **2** and **3**, implies that electron transfer for $[Re_2(CO)_{10}]^{\cdot+}$ proceeds at a rate significantly faster than those for **1**, **2** or **3** if a similar mechanism is operative. A critical factor for the EC second-order disproportionation path might be the potential difference between the first and second oxidation processes. As this value decreases, the rate of the disproportionation should increase. Alternatively, nucleophilic assistance (from solvent or electrolyte anion) may become important for the cationic radical dimers of Mn and Re.

Conclusions

Electrochemical oxidation of $[M_2(CO)_{10}]^{2-}$ (M = Cr, Mo, W) induces metal–metal bond cleavage through an EC second-order disproportionation mechanism, rather than through an ECE mechanism as proposed for related systems. Such mechanisms have been observed for metal–metal bond cleavage in other systems, but usually require ligand assistance [25]. The order of the rates of reaction, W > Mo ≫ Cr, parallels the driving force calculated from the difference between the first and second oxidation potentials. This trend runs counter to that of the metal–metal bond strength, which further supports the proposed mechanism. The activation parameters are also consistent with outer-sphere electron transfer being the rate-limiting step, rather than metal–metal bond cleavage in the radical dimer. An interesting aspect of the $M_2(CO)_{10}^{\cdot-}$ radicals is their relative stability toward nucleophilic attack. In other organometallic radicals facile nucleophilic attack has been attributed to steric accessibility of the odd electron to an incoming nucleophile [24]. In the $M_2(CO)_{10}^{\cdot-}$ radicals the unpaired electron may reside in the metal–metal bonding σ orbital. If that occurs it would be shielded by the axial CO groups from nucleophilic attack so that CO substitution might be slow relative to disproportionation.

Acknowledgement

This work was supported by a National Science Foundation Grant CHE-88-15958.

References

1 M. S. Wrighton and D. Bredesen, *J. Organomet. Chem., 50* (1973) C35–C38.
2 M. S. Wrighton and D. S. Ginley, *J. Am. Chem. Soc., 97* (1975) 2065–2072.
3 S. A. Hallock and A. Wojcicki, *J. Organomet. Chem., 54* (1973) C27–C29.
4 A. G. Osborne and M. H. B. Stiddard, *J. Chem. Soc.,* (1964) 634–636.
5 R. J. Haines, R. S. Nyholm and M. H. B. Stiddard, *J. Chem. Soc. A,* (1968) 43–46.
6 B. H. Byers and T. L. Brown, *J. Am. Chem. Soc., 97* (1975) 3260–3262.
7 D. A. Lacombe, J. E. Anderson and K. M. Kadish, *Inorg. Chem., 25* (1986) 2074–2079.
8 J. R. Pugh and T. J. Meyer, *J. Am. Chem. Soc., 110* (1988) 8245–8246.
9 M. Arewgoda, P. H. Rieger, B. H. Robinson, J. Simpson and S. J. Visco, *J. Am. Chem. Soc., 104* (1982) 5633–5640.
10 C. J. Pickett and D. Pletcher, *J. Chem. Soc., Dalton Trans.,* (1975) 879–886.
11 C. J. Pickett and D. Pletcher, *J. Chem. Soc., Dalton Trans.,* (1976) 749–752.
12 A. M. Bond, J. A. Bowden and R. Colton, *Inorg. Chem., 13* (1974) 602–608.
13 A. M. Bond and R. Colton, *Inorg. Chem., 15* (1976) 446–448.
14 J. K. Kochi, in W. C. Trogler (ed.), *Organometallic Radical Processes,* Elsevier, Amsterdam, 1990, pp. 201–269.
15 R. A. Levenson and H. B. Gray, *J. Am. Chem. Soc., 97* (1975) 6042–6047.
16 R. T. Baker, J. C. Calabrese, P. J. Krusic, M. J. Therien and W. C. Trogler, *J. Am. Chem. Soc., 110* (1988) 8392–8412.
17 J. K. Ruff and W. J. Schlientz, *Inorg. Synth., 15* (1974) 84–90.
18 W. Strohmeier and K. Gerlach, *Chem. Ber., 94* (1961) 398–406.
19 T. L. Brown, in W. C. Trogler (ed.), *Organometallic Radical Processes,* Elsevier, Amsterdam, 1990, pp. 67–107.
20 M. K. Hanafey, R. L. Scott, T. H. Ridgway and C. N. Reilley, *Anal. Chem., 50* (1978) 116–137.
21 K. Kirchner, L.-F. Han, H. W. Dodgen, S. Wherland and J. P. Hunt, *Inorg. Chem., 29* (1990) 4556–4559; K. A. Anderson and S. Wherland, *Inorg. Chem., 30* (1991) 624–629.
22 L. B. Handy, J. K. Ruff and L. F. Dahl, *J. Am. Chem. Soc., 92* (1970) 7312–7326.
23 R. A. Marcus, *Ann. Rev. Phys. Chem., 15* (1964) 155–196.
24 W. C. Trogler, in W. C. Trogler (ed.), *Organometallic Radical Processes,* Elsevier, Amsterdam, 1990, pp. 306–337.
25 J. P. Bullock, M. C. Palazotto and K. R. Mann, *Inorg. Chem., 30* (1991) 1284–1293; N. P. Forbus and T. L. Brown, *Inorg. Chem., 20* (1981) 4343–4337; M. Absi-Halabi, J. D. Atwood, N. P. Forbus and T. L. Brown, *J. Am. Chem. Soc., 102* (1980) 6248–6254; M. Absi-Halabi and T. L. Brown, *J. Am. Chem. Soc., 99* (1977) 2982–2988.